Main Manuscript for
Closed-loop recyclable membranes enabled by covalent adaptable networks for water purification

Bofan Li[1#], Sheng Wang [1#], Xian Jun Loh[1,2,3], Zibiao Li[1,2,3*], Tai-Shung Chung[4*]

[1]Institute of Sustainability for Chemicals, Energy and Environment (ISCE[2]), Agency for Science, Technology, and Research (A*STAR), 1 Pesek Road, Jurong Island, Singapore 627833, Republic of Singapore.

[2]Institute of Materials Research and Engineering (IMRE), Agency for Science, Technology, and Research (A*STAR), 2 Fusionopolis Way, Innovis #08-03, Singapore 138634, Republic of Singapore.

[3]Department of Materials Science and Engineering, National University of Singapore, Singapore 117576, Republic of Singapore.

[4]Graduate Institute of Applied Science and Technology, National Taiwan University of Science and Technology, Taipei 10607, Taiwan.

*Corresponding authors, email: lizb@imre.a-star.edu.sg (Z. Li); chencts@nus.edu.sg, chencts@mail.ntust.edu.tw (T. S. Chung)

[#]B. L and S. W equally contributed to this work

Author Contributions: B. Li and S. Wang conceived the idea, designed the experiments and drafted the manuscript. B. Li fabricated the membranes and conducted the testing and characterizations. S. Wang synthesized the polymer and performed the characterizations. T.S. Chung, Z. Li and X.J. Loh contributed to the project discussions and manuscript writing.

Competing Interest Statement: The authors declare no competing interests.

Classification: Physical Sciences, Engineering

Keywords: Closed-loop recyclable membranes; covalent adaptable networks; sustainable membranes; water purification.

This PDF file includes:

Main Text
Figures 1 to 5

Abstract

In the state-of-the-art membrane industry, membranes have linear life cycles and are commonly disposed of by landfill or incineration, sacrificing their sustainability. To date, little or no thought is given in the design phase to the end-of-life management of membranes. For the first time, we have innovated high-performance sustainable membranes, which can be closed-loop recycled after long-term usage for water purification. By synergizing membrane technology and dynamic covalent chemistry, covalent adaptable networks (CANs) with thermally reversible Diels-Alder (DA) adducts were synthesized and employed to fabricate integrally skinned asymmetric membranes via the non-solvent induced phase separation technique. Due to the stable and reversible features of CAN, the closed-loop recyclable membranes exhibit excellent mechanical properties, thermal and chemical stabilities as well as separation performance, which are comparable to or even higher than the state-of-the-art non-recyclable membranes. Moreover, the used membranes can be closed-loop recycled with consistent properties and separation performance by depolymerization to remove contaminants, followed by refabrication into new membranes through the dissociation and reformation of DA adducts. This study may fill in the gaps in closed-loop recycling of membranes and inspire the advancement of sustainable membranes for a green membrane industry.

Significance Statement

Membranes fabricated in today's membrane industry typically have linear life cycles and are disposed of by landfill or incineration, compromising their sustainability. The novel closed-loop recyclable membrane fabricated from covalent adaptable networks (CANs) can be depolymerized after fouling and refabricated into new membranes with consistently high performance for water purification. It also exhibits excellent mechanical properties, thermal and chemical stabilities as well as separation performance thanks to the stable and reversible features of CANs. The recyclable membrane designed in this work could fill in the gaps of closed-loop recycling in the sustainable and green membrane industry that will ultimately reduce thousands of tons of membrane waste and carbon footprint.

Main Text

Introduction

Water purification is essential in producing drinking water and treating wastewater in pharmaceutical, electrical, and textile industries (1-3). Membrane technology has been intensively implemented in wastewater treatment to remove contaminants for water discharge or to recycle valuable components for reuse (4-10). The vast majority of membranes are made of non-recyclable or non-renewable polymers, which is mainly attributed to the high separation performance as well as the excellent durability and stability required for water separations (11, 12). After long-term usage, the performance of the membranes will decline due to membrane fouling as contaminants in the feed solutions are accumulated on the membrane surface and block the pores. Typically, the lifetimes of reverse osmosis (RO) and nanofiltration (NF) membranes are 3-7 years and they are usually disposed of by landfills or incineration. Over 14,000 tons of RO membranes are discarded annually, and an even higher number of microfiltration (MF) and ultrafiltration (UF) membranes are disposed of, generating a massive amount of CO_2 and sacrificing the sustainability of membranes (13, 14). This has arisen the environmental awareness of membrane researchers to relook the sustainability over the entire life cycle of membranes.

The current life cycle of a membrane is linear, starting from the membrane manufacturing process to the end-of-life membrane management. Based on the twelve principles of green chemistry, a sustainable circular membrane industry is designed where renewable or recyclable polymers and green solvents are employed, its by-product waste is reused, and the old membranes are reused or recycled (11). Up to now, research works have been done on exploring biobased or biodegradable polymers and green solvents (15-17). Some studies have also investigated the reuse of membranes via chemical cleaning or downgrading RO membranes to NF or UF membranes (13, 18). While hardly any studies have been done on recycling membranes due to the difficulties in recycling the contaminated and fouled membranes. In addition, little or no thought is given in the design phase to the end-of-life management of membranes (14). Thus, it is a novel

initiative to design a high-performance membrane with closed-loop recyclability, which will not only solve the membrane disposal issue but also improve the sustainability of the membrane industry.

Covalent adaptable network (CAN) is an emerging class of polymeric materials with crosslinked networks and dynamic covalent bonds that combine the superior properties of thermoplastic and thermoset characteristics (19-25). CANs are extra stable in the application environment, however, the topological network rearrangement and polymer network depolymerization can be achieved when the dynamic bond exchange or dissociation/association is triggered by external stimuli (such as heat, light or pH). CANs are promising to realize the recycling of used membranes and are highly suitable for membrane application by considering the following advantages: i) The covalent crosslinking feature of CANs can provide membranes with excellent mechanical properties, dimensional, thermal and chemical stabilities; ii) The dynamic nature of CANs can endow the membranes with closed-loop recyclability; iii) The viscosity of CANs can be easily regulated by the pre-reaction between the dynamic crosslinking points, adjustable to the requirements of different fabrication methods; iv) The diversified CANs based on different polymers and dynamic bonds/reactions can significantly enrich the family of membranes.

In view of the requirements in membrane fabrication and application process, a temperature-reversible CAN with furan-maleimide Diels-Alder (DA) adducts was selected as the DA reaction can occur at room temperature to avoid destroying the porous structure of the membrane at high temperatures. In addition, the retro-DA reaction follows a dissociation mechanism with low reaction free energies (-8 to -70 kJ mol^{-1}) (26, 27), which provides great convenience for closed-loop recycling. Integrally skinned asymmetric (ISA) membranes were fabricated via the non-solvent induced phase separation (NIPS) method for water purification, exemplified by dye/salt fractionation to treat textile wastewater, where membranes are easy to be fouled by dyes and salt precipitates. For the first time, by combining membrane technology and dynamic covalent chemistry, we have demonstrated an innovative strategy and method to make high-performance, sustainable membranes for water purification, which can be closed-loop recycled after long-term

usage (Fig. 1). This may inspire the advancement of next-generation closed-looped recyclable membranes for a sustainable and green membrane industry that will ultimately reduce thousands of tons of membrane waste and carbon footprint.

Results

Polymer synthesis and membrane fabrication

Considering the high mechanical strength, hydrophilicity and infinite recyclability of the desired membranes, epoxy resins containing ether repeating units synthesized from oligomer/monomer is designed. A 4-arm furan-functionalized oligomer FGE-D230 was firstly synthesized from polyetheramine D-230 (D230) and furfuryl glycidyl ether (FGE), as shown in Fig. S1 (Supporting Information). The successful synthesis of FGE-D230 was confirmed using ^{1}H nuclear magnetic resonance (NMR) by matching the characteristic peaks with H atoms in the desired molecular structure (Fig. S2, Supporting Information). The as-synthesized FGE-D230 was then crosslinked with 1,1′-(Methylenedi-4,1-phenylene) bismaleimide (BMI) in the presence of N, N-dimethylformamide (DMF) and polyethylene glycol (PEG) as the solvent and pore former, respectively (Fig. 2a). By heating the dope solution at 60 °C, the forward DA reaction proceeded with an increase in viscosity, which was monitored against heating time, as shown in Fig. 2b. The viscosity firstly increased linearly with heating time and after a certain point it rose dramatically, displaying a similar trend compared to the viscosity versus polymer concentration profile. Learning from the critical concentration, a critical heating time was identified by locating the crossed point of extrapolation lines of the two linear parts of the viscosity curve (28, 29). To achieve a good chain entanglement and suitable viscosity for membrane casting, this critical heating time was selected to heat the dope prior to cooling the dope in a water bath at room temperature. Subsequently, the membranes were fabricated by immersing the as-cast dope solution in a water bath via the NIPS method.

The DA reaction between FGE-D230 and BMI was confirmed by Fourier transform infrared spectroscopy (FTIR) under the attenuated total reflectance (ATR) mode, as shown in Fig. 2c. The

FTIR spectrum of FGE-D230 possesses a characteristic peak of furan ring breathing at around 1016 cm^{-1}, while the representative peak of =C-H bending in maleimide groups appears at 688 cm^{-1} in the FTIR spectrum of BMI. The successful crosslinking between FGE-D230 and BMI is confirmed by the formation of DA adduct, where a stretching vibration peak of C=O of DA adduct shows at 1775 cm^{-1}. At the same time, the characteristic peaks of the furan ring and maleimide group disappear in the FTIR spectrum of the prepared membrane. These indicate the majority of FGE-D230 and BMI have been crosslinked to form CAN via DA reaction in the membrane fabrication process (30, 31). To further characterize the crosslinking degree of the prepared membrane, the gel contents of the prepared membrane were measured by the change of membrane mass before and after immersion in ethanol, dichloromethane and DMF at room temperature for 3 days. The gel contents of the CAN membrane in all three selected solvents are above 94% (Fig. 2d), which indicates the formation of a highly crosslinked network. The high crosslinking degree endows the membrane with excellent stability in harsh solvents (Fig. S3, Supporting Information). In particular, the membrane is stable in strong acid and alkaline solutions, which shows good applicability and durability for water purification.

Thermal and mechanical properties

The thermal and mechanical properties of the newly developed membrane were characterized to ensure its industrial applicability and scalability. Figure 2e displays the differential scanning calorimetry (DSC) thermograph of the prepared membrane. The glass transition temperature (T_g) of the CAN is determined to be 89 °C, which is considerably high enough for water purification. The retro DA reaction starts at 110 °C (Fig. 2e) (32), which is higher than the boiling point of water under standard conditions. This guarantees the stability of the CAN membrane to be operated at relatively high temperatures. In addition, the temperature-reversible DA cycloaddition reaction based on the furan-maleimide structure was investigated by a real-temperature FTIR spectroscopy (Fig. 2f). The C=O stretching vibration in DA adduct at ~1775 cm^{-1} was monitored to characterize the dissociation degree of DA adduct at different temperatures ranging from 70 °C to 160 °C. The peak intensity of C=O remains almost the same at low temperatures of 70 – 100 °C and it starts to drop at 110 °C,

indicating the dissociation reaction becomes dominant at temperatures above 110 °C. The peak intensity further decreases remarkably with an increase in temperature until the temperature reaches 150 °C, after which the peak intensity no longer decreases significantly with a further increase in temperature. In addition, the thermal stability of the CAN membrane was evaluated by the thermogravimetric analysis (TGA) test, as shown in Fig. S4 (Supporting Information). The initial degradation temperature for 5% weight loss ($T_{d5\%}$) and char yield at 700 °C is 282 °C and 33%, respectively, which suggests excellent thermal stability for membrane separations.

The mechanical properties of the CAN membrane were further determined by tensile tests and the stress versus strain plot is plotted in Fig. 2g. The young's modulus, tensile strength and elongation at break are 150.58±14.40 MPa, 1.59±0.08 MPa and 4.07±0.03 %, respectively. This is comparable to typical ISA membranes made from polyethersulfone and polyvinylidene fluoride in the literature (33, 34). In addition, the as-cast CAN membrane demonstrates excellent flexibility that can be curled and assembled into membrane modules (Fig. 2g). The excellent tensile resistance and flexibility make the membrane highly promising to be scaled up and industrialized.

Membrane morphology and surface properties

The top surface, bottom surface and cross-section of the CAN membrane were observed by a field emission scanning electron microscope (FESEM), as displayed in Fig. 3 a-f. The top surface is relatively smooth with a few nodules and small holes on it. In comparison, the bottom surface is slightly rough with small nodular humps, which are possibly formed due to the effect of water intrusion. The cross-section of the membrane contains finger-like macrovoids, which are caused by the rapid phase inversion process and fast solvent-nonsolvent exchange rate (29, 35, 36). This highly porous membrane structure reduces the transport resistance in the membrane sublayer and is highly beneficial for water transport. From the cross-sectional image, the membrane thickness is determined to be around 130 μm. The magnified top cross-section displays a dense selective layer on top of the porous substructure. The thickness of this dense selective layer was analyzed using a transmission electron microscopy (TEM) and determined to be 137.9 ± 12.1 nm (Fig. S5,

Supporting Information). This dense skin layer is critical to retaining organic solutes in water. In the middle part of the cross-section, the finger-like structure is arranged uniformly with polymer nodules and interconnected pores. The interconnected pore can further reduce membrane resistance and promote the transport of water molecules. The bottom part of the membrane's cross-section is very porous with large finger-like macrovoids. The open and interconnected polymer network can facilitate the passage of water molecules. An ISA membrane with a morphology consisting of a dense skin layer and a sub porous layer is promising to achieve both high flux and high rejection (37).

The surface hydrophilicity was characterized by a goniometer. The membrane is hydrophilic with a water contact angle of 49.4 ± 2.4° (Fig. 3g), owing to the hydroxyl groups and ether groups in FGE-D230 as well as the polar DA adduct. The hydrophilic membrane surface has low surface energy and is beneficial for water molecules to enter membrane pores. In order to interpret the separation performance of the prepared CAN membrane, the surface zeta potential was measured at different pH conditions (Fig. 3h). The membrane possesses an isoelectric point of ~4.3, which means that the membrane has a slightly positive charge below pH 4.3 and becomes negatively charged at higher pH values. This is attributed to the various functional groups of FGE-D230 and BMI, such as hydroxyl groups, ether groups, tertiary amine and DA adduct (38). The surface roughness was evaluated by atomic force microscopy (AFM) under the tapping mode. The membrane surface is quite smooth with an average roughness (R_a) of 4.23 ± 0.36 nm. The hydrophilic and smooth characteristics are beneficial for the membrane surface with enhanced antifouling property (39).

Effect of polymer composition on separation performance

The separation performance of the membranes was evaluated by water permeance and rejection towards a dye, fast green FCF (FG). The type of monomers was first studied by varying the structural length of the prepolymer FGE-D230 using either a shorter-chain diethylenetriamine (TAEA) or a longer-chain polyetheramine D-400 (D400) to replace D230. The TAEA-based membrane has a water permeance much higher than the D230-based membrane with a slightly

lower rejection (Fig. S6, Supporting Information). In contrast, the D400-based membrane possesses a very low water permeance and rejection. This phenomenon can be explained by their membrane morphologies, as displayed in Fig. S7 (Supporting Information). The TAEA-based membrane consists of a very thin selective layer and a porous sublayer, especially its top surface contains many holes and nodules. This leads to have a low resistance for water and dye molecules to transport through the membrane. The selective layer of the D400-based membrane is thick but there are a lot of voids in the selective layer. There are also small pores inside the finger-like macrovoid structure, resulting in a soft and compressible membrane structure. Thus, its low water flux may result from pore collapse and structure compaction under high-pressure filtration. At the same time, the dye molecules cannot be retained by the membrane due to its loose and defective skin layer, leading to both low water permeance and low rejection.

The effect of pore former is also investigated by varying the molecular weight of PEG and the results are displayed in Fig. S8 (Supporting Information). The water permeance dramatically increases with a decreased dye rejection as the molecular weight of PEG increases. This is mainly due to the micropores generated during the phase inversion process, where PEG molecules leach out from the solidified membrane to the non-solvent coagulant and create micropores in the membrane matrix. As the PEG molecular weight increases, the created micropores become larger, resulting in a higher water permeance and a lower rejection. In addition, the selective layers of the three membranes may also play a role in separation performance, as shown in Fig. S9 (Supporting Information). The selective layer of the PEG400-based membrane is very dense with a smooth surface, whereas the skin layer of the PEG1k-based membrane is much porous and its surface contains small holes.

Furthermore, the dope composition was tuned and adjusted to optimize the separation performance. Based on the prior results, D230 and PEG were chosen as the prepolymer and pore former, respectively. The weight ratio of polymer, PEG600 and DMF was varied to study the effects of solvent and pore former, as displayed in Fig. S10 and S11 (Supporting Information), respectively.

The water permeance increases with a decreased dye rejection as the weight percentage of the solvent or pore former increases. Notably, the water permeance increases more significantly with an increase in pore former content than that with solvent content. This may be ascribed to the differences in their molecular sizes and viscosity. During the phase inversion process, both solvent and pore former exchange with non-solvent quickly, generating pores and voids in the polymer matrix (29). As DMF has a smaller molecule size and a lower viscosity than PEG600, the latter results in larger pores than the former in the selective layer when they leach out of the membranes. Therefore, an increase in PEG600 content in dope solutions has greater impact on permeance increase and rejection decrease than that in DMF. Based on the separation performance, the ratio of 1:1:0.7 (i.e., polymer: pore former: solvent) is chosen for the subsequent studies.

Separation performance for dye/salt fractionation

The water permeance and rejection towards single salt were firstly determined using 1000 ppm of NaCl, Na_2SO_4, $MgCl_2$, $MgSO_4$ solutions as feed solutions at 1 bar. The pure water permeance of the CAN membrane is 28.5 L m^{-2} h^{-1} bar^{-1} (LMH bar^{-1}), which falls in the range of nanofiltration to ultrafiltration. As shown in Fig. 4a, the CAN membrane has relatively low rejections to the four salts, mainly because of its relatively loose structure and large pore size. The rejection towards $MgCl_2$ is the highest, followed by $MgSO_4$, Na_2SO_4 and the rejection towards NaCl is the lowest, which is only 3.5%. This phenomenon may arise from the combined effects of size sieving and Donnan exclusion, but the former is dominant as the membrane possesses a close-to-neutral charge at neutral pH. The low salt rejection offers great potential to treat high-salinity wastewater in the textile industry, where NaCl and Na_2SO_4 are usually added at high concentrations to enhance the adhesion of dyes to the fabrics and to maximize the exhaustion of dye molecules (40, 41). To further determine the ability of the CAN membrane for dye removal, various dye solutions were prepared as feed solutions for filtration tests at 1 bar. Table S1 summarizes the properties and molecular structures of the selected dyes. Rejections towards these dyes increase with the molecular weight of the dyes, as displayed in Fig. 4b, and a trendline is plotted to guide the view. To characterize the pore size distribution and determine the molecular weight cut-off (MWCO) of

the newly developed CAN membrane, the membrane rejections towards PEGs with different molecular weights were measured. The pore size distribution is shown in Fig. S12 (Supporting Information) and the MWCO, where 90% of the solute is rejected, is determined to be 4581 g mol^{-1}. This is higher than the molecular weights of dyes, which is mainly attributed to the aggregation of dyes as clusters with enhanced sizes and low diffusivity (42, 43).

A long-term performance test was conducted continuously using a mixed dye/salt solution for 100 h to study the stability of CAN membranes under simulated industrial conditions. Figure 4c shows the variation of water permeance and rejections towards NaCl and FG as a function of time. The water permeance slightly decreases during the first 36 h, possibly due to the membrane compaction and fouling phenomenon. The dye molecules may be easily absorbed by the membrane matrix since the condition is used to dye fabrics in the dye/salt mixture. A stable water permeance is achieved after the fouling phenomenon reaches saturation. The rejections towards the dyes and salts are very stable during the 100-h test, indicating its good stability in separating textile wastewater. The water permeance and separation factor, which is defined as the ratio of dye to salt in the permeant to that in the feed, is computed and compared with reported membranes in the literature (Fig. 4d and Table S2, Supporting Information). The separation factor evaluates the membrane's ability to separate dyes and salts in a mixed solution. A higher separation factor indicates a better separation performance for dye and salt mixtures, which is in favor of treating textile wastewater. Figure 4d suggests that the newly developed CAN membrane possesses an excellent dye/salt fractionation performance, which surpasses or at least comparable to most NF and UF membranes in the literature (Table S2, Supporting Information). Some NF and UF membranes in this table are commercially available membranes and most are lab-scale ISA and TFC membranes fabricated by phase inversion techniques, interfacial polymerization, coating and/or deposition methods.

Closed-loop recyclability

As aforementioned, dye molecules can easily be adsorbed onto the membrane in textile wastewater, which results in the fouling phenomenon by blocking membrane pores and sacrificing permeability. It is difficult to remove the adsorbed dyes by physical and chemical cleaning due to the strong adhesion between dye molecules and membranes (44, 45). To solve this problem, the closed-loop recyclable membrane is designed to be depolymerized to get rid of the dyes and other contaminants prior to refabrication and reuse. The recyclability of the newly developed membranes is demonstrated by depolymerizing the used membranes through a retro-DA reaction at 140 °C (Fig. 5a). Briefly, the depolymerized oligomer solution was firstly filtered through filter papers to remove large foulants such as solids and mineral precipitates, while small foulants such as dyes and inorganic salts were separated by means of a liquid extraction method. As the small dyes and salts were highly soluble in water, they could be extracted from the aqueous phase while the oligomers remained in the oil phase. After the oligomer solution was separated from the foulants, the recycled oligomers were obtained by evaporating the solvents and then were refabricated into a new membrane via DA reaction and phase inversion technique for reuse. The membrane morphology of the original, 1st recycled and 2nd recycled membranes were observed by FESEM (Fig. 5b). The top surfaces possess similar smooth morphology with a few nodules and tiny holes on them. The cross-sections and selective layers of the membranes remain almost the same after recycling, suggesting that CAN membranes can be recycled and refabricated with a similar morphology and structure.

To evaluate the performance of the recycled membranes, the thermal, mechanical and separation performance of the original, 1st recycled and 2nd recycled membranes were measured and compared. The chemical structures of the original and recycled membranes were confirmed by FTIR as displayed in Fig. 5c. The FTIR spectra of the original, 1st recycled and 2nd recycled membranes are almost the same with the DA adduct peak showing at ~1775 cm^{-1}. In addition, the peak location and intensity of the major peaks are also the same for the three membranes, indicating the contents of the membrane remain unchanged after each recycling process. Figure 5d shows their thermal properties by measuring their DSC curves. The T_g of the membranes is

slightly increased by the recycling process. Nevertheless, the retro DA reaction of the three membranes occurs at the same location, demonstrating the consistent recyclability of CAN membranes after several recycling processes. In addition, the mechanical properties of the original and recycled membranes were characterized by tensile tests (Fig. 5e). The tensile strength and Young's modulus increase with a decreased elongation at break, suggesting the membrane becomes stiff during the recycling process. This is a common phenomenon observed in recycled and reprocessed polymers due to the side reactions (e.g. oxidation of benzene rings and double bonds, self-polymerization of double bonds) during the high-temperature recycling process as evidenced by extensive research studies (46, 47). In addition, the separation performance of the original and recycled membranes was examined by water permeance and dye rejection (Fig. 5f and Fig. S13, Supporting Information). The water permeance and dye rejection of the recycled membranes remain comparable to those of the original membranes for at least three cycles, despite a slight decrease in water permeance. The consistent properties and separation performance demonstrate the feasibility of the closed-loop recycled membranes for water purification.

Discussion

Different from the state-of-the-art membranes with linear life cycles, the CAN membranes in this work can be closed-loop recycled via depolymerization and refabrication after long-term usage. From the viewpoint of dynamic covalent chemistry, the reversible DA cycloaddition is responsive to temperature, where the DA adduct forms at low temperatures and dissociates at above 90°C. The viscosity of CAN solutions can be easily regulated by the pre-reaction between the dynamic crosslinking point, which is essential to fabricating ISA membranes via NIPS technique. The low free energy of dissociation and catalyst-free properties also provide a great convenience for membrane fabrication and closed-loop recycling. Moreover, the crosslinked nature of CANs endows the membrane with excellent thermal properties, mechanical robustness and flexibility, chemical stabilities as well as high performance for up-scaled liquid separations. Therefore, the newly developed CAN membranes with high performance and closed-loop recyclability are highly potential to be applied for industrial separation processes. Herein, the wastewater from the textile

industry containing high concentrations of dyes and inorganic salts is treated by the CAN membrane for dye/salt fractionation. The CAN membrane possesses a water permeance of 28.5 LMH bar^{-1} and an MWCO of 4581 g mol^{-1}, which could almost retain dyes, including FG, RB and AB8X, with only 3.5% rejection towards NaCl. However, dyes tend to be absorbed onto the membrane matrix in the presence of high concentrations of salts, resulting in a decline in separation performance. Backwashing and chemical cleaning cannot effectively remove the fouling and scaling under this condition. The newly developed recyclable membrane is demonstrated to be depolymerized to remove the contaminates, followed by refabrication into new membranes via reversible DA reaction. The chemical, mechanical and thermal properties as well as separation performance of the recycled CAN membranes remain consistent after recycling for two or even more times, exhibiting excellent recyclability. The recyclable membranes designed in this work could fill in the gaps of closed-loop recycling in the sustainable and green membrane industry that will ultimately reduce thousands of tons of membrane waste and carbon footprint. It can also expand the horizons for the transition of the membrane industry from linear to circular and positively impact the net zero emission goal of the Paris Agreement.

Materials and Methods

Preparation of CAN membranes

The 4-arm furan-functionalized oligomer FGE-D230 was firstly synthesized by reacting polyetheramine D-230 and furfuryl glycidyl ether in a vial under argon at 80 °C for 6 h, followed by heating at 120 °C for 2 h. The obtained FGE-D230 was then preserved in an argon environment for further usage. To prepare the dope for membrane fabrication, FGE-D230 and BMI were added to a vial with a molar ratio of 1:0.9, along with certain amounts of PEG and DMF. The weight ratio of polymer, PEG and DMF was adjusted to tune the membrane structure and optimize the membrane performance. In order to enhance the mixing, the dope was firstly heated at 140 °C for 3 mins with vigorous shaking, followed by rapid cooling in an ice water bath. After that, the mixture was heated at 60 °C to promote the forward crosslinking reaction until the viscosity reached a state that allowed for proper casting. The mixture was then removed from the hotplate and rapidly cooled

in a water bath at room temperature. The CAN membranes were fabricated by casting the dope using a casting knife with an air gap of 150 μm on a PVA-coated glass plate, prior to phase inversion in a DI water bath for at least 1 day to complete the phase inversion. The PVA coating was conducted using a wire rod coater to facilitate the detachment of membranes.

Membrane performance

The pure water permeance (PWP, L m^{-2} h^{-1} bar^{-1}, LMH bar^{-1}) of the membrane was measured using dead-end filtration cells with a trans-membrane pressure ΔP (bar) of 1 bar at room temperature. The PWP was calculated using the following equation:

$$PWP = \frac{Q}{A\Delta P} \quad (1)$$

where Q (L h^{-1}) is the water flux at the permeate side and A (m^2) is the effective filtration area of the membrane. Each membrane sample was assembled and stabilized for 1 h before taking any measurement. At least three membrane samples were measured for each condition to ensure reproducibility and the average results were reported.

The rejections to dyes and inorganic salts were determined using feed solutions containing 50 ppm dyes or 1000 ppm inorganic salts under a trans-membrane pressure of 1 bar with pre-stabilization of 1 h. The concentrations of dye and salt in both feed (C_f) and permeate (C_p) were measured using a UV-Vis spectrophotometer (UV-1800 UV/visible Scanning spectrophotometer, Shimadzu) and a conductivity meter (SevenCompact, Mettler-Toledo), respectively. The dye and salt rejections (R, %) were calculated using Eq. (2).

$$R = \left(1 - \frac{C_p}{C_f}\right) \times 100\% \quad (2)$$

The dye/salt fractionation test was conducted using mixed feed solutions consisting of 50 ppm FG and 1000 ppm NaCl under 1 bar for 100 h. The separation factor of dye and salt was determined using the following equation.

$$Separation\ factor_{\frac{Salt}{Dye}} = \frac{x_{Salt}^{permeant} / x_{Dye}^{permeant}}{x_{Salt}^{feed} / x_{Dye}^{feed}} \quad (3)$$

Closed-loop recycling

After filtration with dyes and salts, the used membranes were depolymerized through a retro-DA reaction at high temperatures. The used membranes were heated at 140 °C in DMF for 15 mins to induce the depolymerization reaction. After depolymerization, the solid membranes became a liquid mixture with dissolved oligomers and foulants in DMF. The mixture was first filtered through a filter paper to remove any large foulants, such as sands and mineral precipitates. To separate oligomers from dyes and salts, a liquid extraction method was employed due to the large difference in their solubility. An equal amount of DCM and water were added to the mixture with vigorous shaking. The oligomers were soluble in the DCM phase, while DMF, dyes and salts were extracted in the aqueous phase as they were highly soluble in water. The recycled oligomers could then be obtained by evaporating the solvents and be refabricated into a new membrane as described in section 4.2. The same batch membranes were recycled and refabricated twice with property and performance characterizations to validate the closed-loop recyclability of the developed CAN membrane.

Acknowledgments

The authors would like to acknowledge the financially supported from the Agency for Science, Technology and Research (A*STAR) under its A*STAR Career Development Fund – Seed Project 2022 for the project entitled “Closed-loop recyclable membranes for circular membrane industry” (Grant No. C222812032), UGT HTPO for the project entitled, “Transforming Commodity Chemicals into Vitrimeric Materials for Circular Plastics” (Grant No. C211718004), RIE2025 Manufacturing, Trade and Connectivity (MTC) Programmatic Funding (M22K9b0049), and AME Young Individual Research Grants (YIRG) for the project entitled, “Vitrimers from Waste Plastics (V-WASP)” (Grant No. A2084c0168). Special thanks are due to Ms. Koh Xue Qi and Dr. Tan Hui Ru for their kind assistance in this study.

References

1. M. A. Shannon *et al.*, Science and technology for water purification in the coming decades. *Nature* **452**, 301-310 (2008).
2. Z. Tan, S. Chen, X. Peng, L. Zhang, C. Gao, Polyamide membranes with nanoscale Turing structures for water purification. *Science* **360**, 518-521 (2018).
3. M. Peydayesh, R. Mezzenga, Protein nanofibrils for next generation sustainable water purification. *Nat. Commun.* **12**, 3248 (2021).
4. R. W. Baker, *Membrane technology and applications* (John Wiley and Sons Ltd, United Kingdom, ed. 3rd, 2012).
5. S. Guo, Y. Wan, X. Chen, J. Luo, Loose nanofiltration membrane custom-tailored for resource recovery. *Chem. Eng. J.* **409**, 127376 (2021).
6. B. Li, S. Japip, T. S. Chung, Molecularly tunable thin-film nanocomposite membranes with enhanced molecular sieving for organic solvent forward osmosis. *Nat. Commun.* **11**, 1198 (2020).
7. Y. Lu *et al.*, Monolayer graphene membranes for molecular separation in high-temperature harsh organic solvents. *Proc. Natl. Acad. Sci. U.S.A.* **118**, e2111360118 (2021).
8. M.-L. Liu *et al.*, Multi-component separation of small molecular/ionic pollutants with smart pH-gating membranes. *Chem. Eng. Sci.* **245**, 116854 (2021).
9. Y. Wang *et al.*, Nanocapsule controlled interfacial polymerization finely tunes membrane surface charge for precise molecular sieving. *Chem. Eng. J.* **409**, 128198 (2021).
10. D. Yu *et al.*, Recent Advances in Stimuli-Responsive Smart Membranes for Nanofiltration. *Adv. Funct. Mater.* **n/a**, 2211983 (2022).
11. W. Xie *et al.*, Toward the next generation of sustainable membranes from green chemistry principles. *ACS Sustainable Chem. Eng.* **9**, 50-75 (2021).
12. Y. Zhang *et al.*, Molecularly soldered covalent organic frameworks for ultrafast precision sieving. *Sci. Adv.* **7**, eabe8706 (2021).
13. W. Lawler *et al.*, Towards new opportunities for reuse, recycling and disposal of used reverse osmosis membranes. *Desalination* **299**, 103-112 (2012).

14. S. P. Nunes *et al.*, Thinking the future of membranes: Perspectives for advanced and new membrane materials and manufacturing processes. *J. Membr. Sci.* **598**, 117761 (2020).

15. F. Galiano *et al.*, Advances in biopolymer-based membrane preparation and applications. *J. Membr. Sci.* **564**, 562-586 (2018).

16. A. Figoli *et al.*, Towards non-toxic solvents for membrane preparation: a review. *Green Chem.* **16**, 4034-4059 (2014).

17. S.-H. Park *et al.*, Hydrophobic thin film composite nanofiltration membranes derived solely from sustainable sources. *Green Chem.* **23**, 1175-1184 (2021).

18. W. Lawler *et al.*, Production and characterisation of UF membranes by chemical conversion of used RO membranes. *J. Membr. Sci.* **447**, 203-211 (2013).

19. P. R. Christensen, A. M. Scheuermann, K. E. Loeffler, B. A. Helms, Closed-loop recycling of plastics enabled by dynamic covalent diketoenamine bonds. *Nat. Chem.* **11**, 442-448 (2019).

20. J. M. García *et al.*, Recyclable, strong thermosets and organogels via paraformaldehyde condensation with diamines. *Science* **344**, 732-735 (2014).

21. P. Shieh *et al.*, Cleavable comonomers enable degradable, recyclable thermoset plastics. *Nature* **583**, 542-547 (2020).

22. M. Podgórski *et al.*, Toward Stimuli-Responsive Dynamic Thermosets through Continuous Development and Improvements in Covalent Adaptable Networks (CANs). *Adv. Mater.* **32**, 1906876 (2020).

23. S. Billiet *et al.*, Triazolinediones enable ultrafast and reversible click chemistry for the design of dynamic polymer systems. *Nat. Chem.* **6**, 815-821 (2014).

24. M. Röttger *et al.*, High-performance vitrimers from commodity thermoplastics through dioxaborolane metathesis. *Science* **356**, 62-65 (2017).

25. N. Zheng, Y. Xu, Q. Zhao, T. Xie, Dynamic covalent polymer networks: A molecular platform for designing functions beyond chemical recycling and self-healing. *Chem. Rev.* **121**, 1716-1745 (2021).

26. B. Briou, B. Améduri, B. Boutevin, Trends in the Diels–Alder reaction in polymer chemistry. *Chem. Soc. Rev.* **50**, 11055-11097 (2021).

27. J. M. Winne, L. Leibler, F. E. Du Prez, Dynamic covalent chemistry in polymer networks: a mechanistic perspective. *Polym. Chem.* **10**, 6091-6108 (2019).

28. N. Peng, T. S. Chung, K. Y. Wang, Macrovoid evolution and critical factors to form macrovoid-free hollow fiber membranes. *J. Membr. Sci.* **318**, 363-372 (2008).

29. T. S. Chung, S. K. Teoh, X. Hu, Formation of ultrathin high-performance polyethersulfone hollow-fiber membranes. *J. Membr. Sci.* **133**, 161-175 (1997).

30. X. Kuang *et al.*, Magnetic dynamic polymers for modular assembling and reconfigurable morphing architectures. *Adv. Mater.* **33**, 2102113 (2021).

31. Q. Li *et al.*, Biosourced acetal and Diels–Alder adduct concurrent polyurethane covalent adaptable network. *Macromolecules* **54**, 1742-1753 (2021).

32. X. Chen *et al.*, A thermally re-mendable cross-linked polymeric material. *Science* **295**, 1698-1702 (2002).

33. E. Elele *et al.*, Mechanical properties of polymeric microfiltration membranes. *J. Membr. Sci.* **591**, 117351 (2019).

34. K. Wang, A. A. Abdalla, M. A. Khaleel, N. Hilal, M. K. Khraisheh, Mechanical properties of water desalination and wastewater treatment membranes. *Desalination* **401**, 190-205 (2017).

35. D.-M. Wang, J.-Y. Lai, Recent advances in preparation and morphology control of polymeric membranes formed by nonsolvent induced phase separation. *Curr. Opin. Chem. Eng.* **2**, 229-237 (2013).

36. G. R. Guillen, Y. Pan, M. Li, E. M. V. Hoek, Preparation and characterization of membranes formed by nonsolvent induced phase separation: A review. *Ind. Eng. Chem. Res.* **50**, 3798-3817 (2011).

37. T. S. Chung, Y. Feng, (editors), *Hollow fiber membranes: fabrication and applications*. T. S. Chung, Y. Feng, Eds. (Elsevier, 2021), https://doi.org/10.1016/C2019-0-03658-8.

38. M. Elimelech, W. H. Chen, J. J. Waypa, Measuring the zeta (electrokinetic) potential of reverse osmosis membranes by a streaming potential analyzer. *Desalination* **95**, 269-286 (1994).

39. X. Li, A. Sotto, J. Li, B. Van der Bruggen, Progress and perspectives for synthesis of sustainable antifouling composite membranes containing in situ generated nanoparticles. *J. Membr. Sci.* **524**, 502-528 (2017).

40. G. Han, T. S. Chung, M. Weber, C. Maletzko, Low-pressure nanofiltration hollow fiber membranes for effective fractionation of dyes and inorganic salts in textile wastewater. *Environ. Sci. Technol.* **52**, 3676-3684 (2018).

41. H.-F. Xiao *et al.*, Amphibian-inspired amino acid ionic liquid functionalized nanofiltration membranes with high water permeability and ion selectivity for pigment wastewater treatment. *J. Membr. Sci.* **586**, 44-52 (2019).

42. M. Hu *et al.*, Selective separation of dye and salt by PES/SPSf tight ultrafiltration membrane: Roles of size sieving and charge effect. *Sep. Purifi. Technol.* **266**, 118587 (2021).

43. J. Zheng *et al.*, Separation of textile wastewater using a highly permeable resveratrol-based loose nanofiltration membrane with excellent anti-fouling performance. *Chem. Eng. J.* **434**, 134705 (2022).

44. B. Van der Bruggen, G. Cornelis, C. Vandecasteele, I. Devreese, Fouling of nanofiltration and ultrafiltration membranes applied for wastewater regeneration in the textile industry. *Desalination* **175**, 111-119 (2005).

45. W.-J. Lau, A. F. Ismail, Polymeric nanofiltration membranes for textile dye wastewater treatment: Preparation, performance evaluation, transport modelling, and fouling control — a review. *Desalination* **245**, 321-348 (2009).

46. S. Wang *et al.*, Facile in situ preparation of high-performance epoxy vitrimer from renewable resources and its application in nondestructive recyclable carbon fiber composite. *Green Chem.* **21**, 1484-1497 (2019).

47. H. Feng *et al.*, Upcycling of dynamic thiourea thermoset polymers by intrinsic chemical strengthening. *Nat. Commun.* **13**, 397 (2022).

Figures

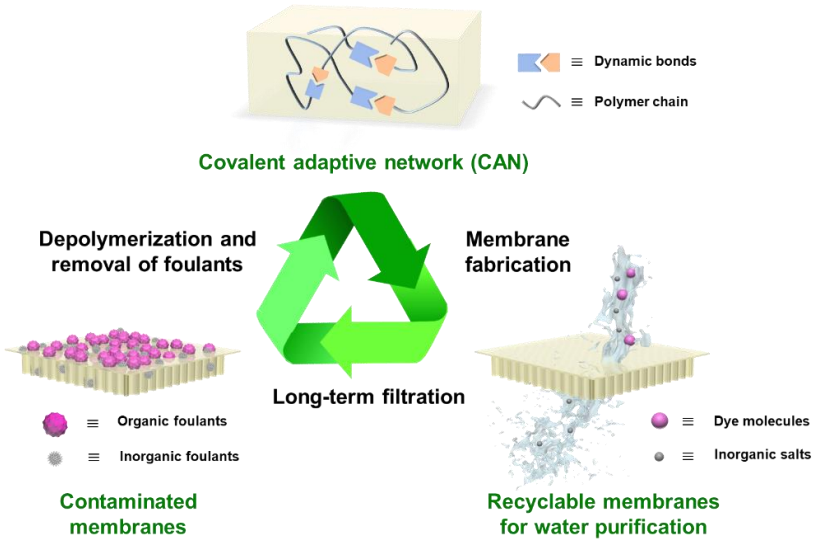

Figure 1. Schematic illustration of the recycling process for the closed-loop recyclable membranes.

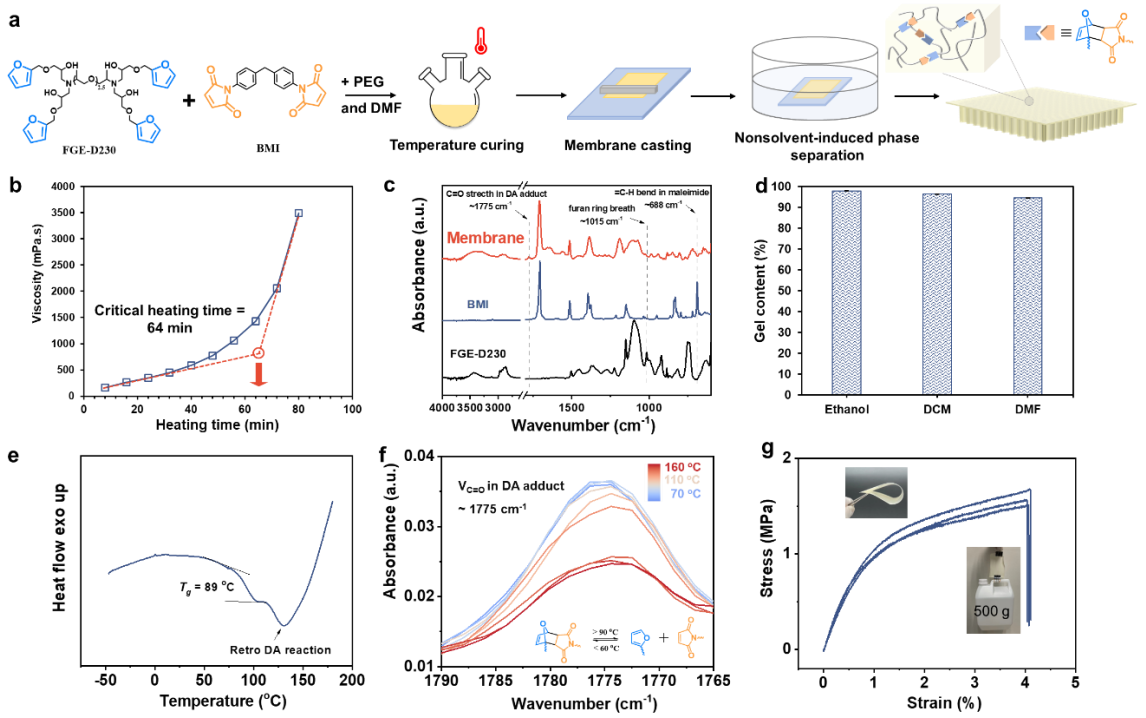

Figure 2. Membrane fabrication and the chemical, thermal and mechanical characterizations of recyclable CAN membranes. a) Schematic illustration of the membrane fabrication process for recyclable CAN membrane. b) The viscosity of CAN dope versus heating time at 60 °C. the critical heating time is determined to be 64 min for membrane casting. c) FTIR spectra of FGE-D230, BMI and the as-cast membrane. d) Gel content of the CAN membrane determined by immersing in ethanol, DCM, DMF for 3 days. e) DSC thermograph of the CAN membrane. f) Real-temp FTIR spectra of the C=O stretching vibration in DA adduct. g) Stress versus strain plot measured by tensile testing.

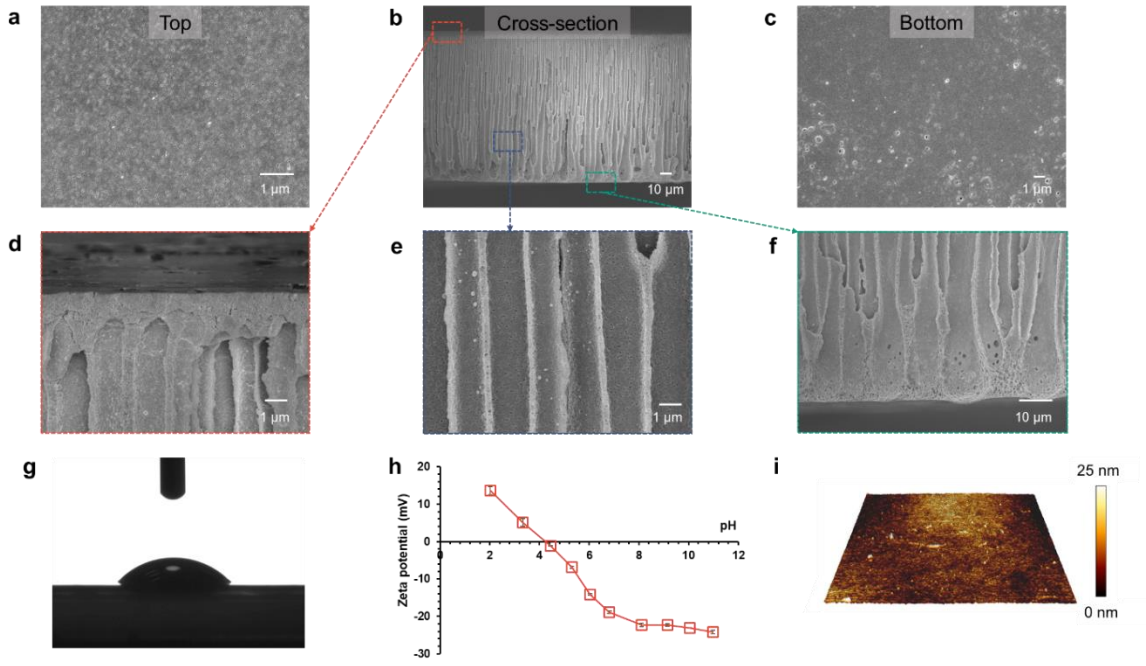

Figure 3. Membrane morphology and surface properties. a)-f) FESEM images of prepared CAN membranes. g) Water contact angle, h) surface zeta potential and i) surface roughness of the CAN membranes.

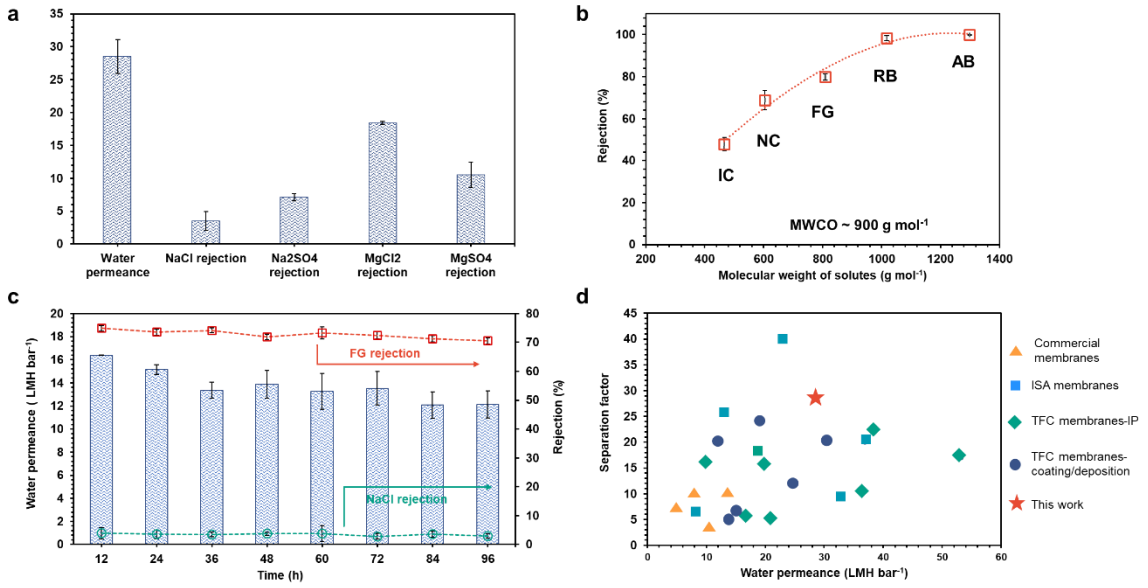

Figure 4. The separation performance of the developed CAN membrane for dye/salt fractionation. a) The pure water permeance and single salt rejection of the CAN membrane. b) The rejections towards selected dyes, i.e., indigo carmine (IC), new coccine (NC), fast green FCF (FG), rose bengal (RB) and Alcian blue 8GX (AB). The rejection is plotted against the molecular weight. c) The water permeance, rejection towards dye and salt as a function of time in a 100-h long-term test for separating stimulated textile wastewater. d) The performance comparison between the developed CAN membranes and reported loose NF membranes.

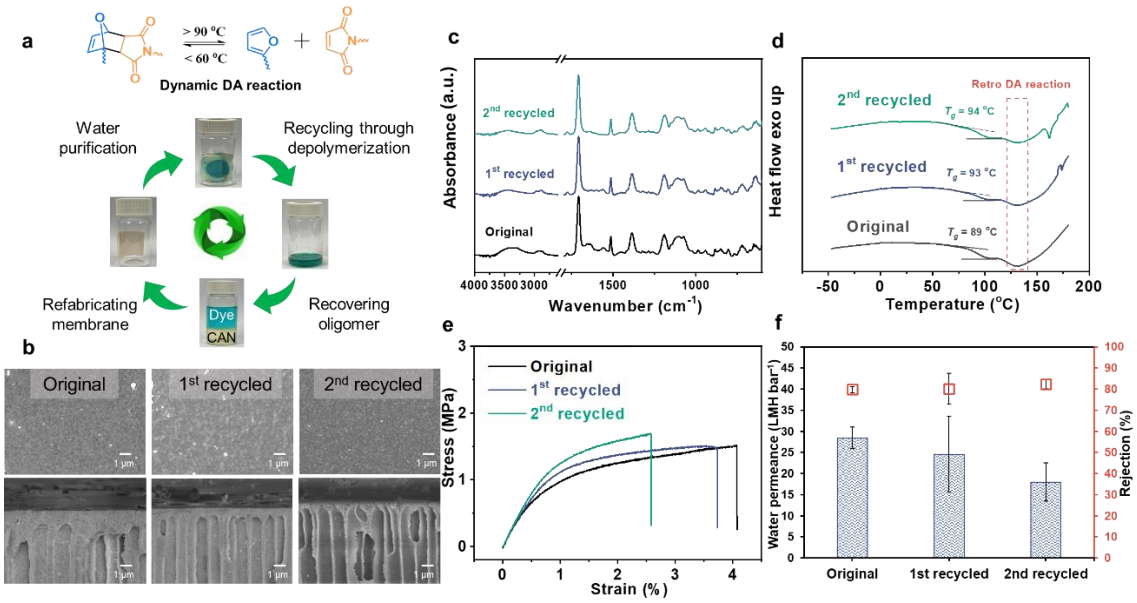

Figure 5. The recyclability of the developed CAN membrane. a) The schematic recycling route b) Top surfaces and cross-sections, b) crosslinking chemistry, c) thermal properties, d) mechanical properties, and e) separation performance of the original and recycled CAN membranes.